Cross sections for transfer of rotational angular momentum in CO_2 from ^{13}C spin relaxation studies in the gas phase

Cynthia J. Jameson
Department of Chemistry, University of Illinois at Chicago, Chicago, Illinois 60680

A. Keith Jameson
Department of Chemistry, Loyola University, Chicago, Illinois 60626

Nancy C. Smith
Department of Chemistry, University of Illinois at Chicago, Chicago, Illinois 60680

Karol Jackowski
Department of Chemistry, University of Warsaw, Warsaw, Poland

(Received 8 October 1986; accepted 18 November 1986)

Nuclear spin-lattice relaxation times (T_1) have been measured for ^{13}C in $^{13}C^{16}O_2$ in pure CO_2 gas and in CH_4, N_2, Ar, HCl, Kr, Xe, and SF_6 gases as a function of temperature. The relaxation is completely dominated by the spin-rotation mechanism so that empirical values of the cross sections for rotational angular momentum transfer σ_J are obtained as a function of temperature. At 300 K the values of $\sigma_J/\text{Å}^2$ are 59.9 ± 0.8 (CO_2–CO_2), 30 ± 1 (CO_2–CH_4), 26.6 ± 0.8 (CO_2–N_2), 33.9 ± 0.2 (CO_2–Ar), 53.5 ± 0.9 (CO_2–HCl), 49 ± 1 (CO_2–Kr), 62 ± 2 (CO_2–Xe), and 91 ± 3 (CO_2–SF_6). The temperature dependence of these cross sections in CO_2–CO_2, CO_2–HCl, CO_2–Xe, and CO_2–SF_6 is T^{-1} as expected, and deviates from T^{-1} in CO_2–CH_4, CO_2–N_2, CO_2–Ar, and CO_2–Kr.

INTRODUCTION

Investigations involving the nonreactive collisions between two molecules require information about the dependence of the potential on molecular reorientation. The latter information has become available by theoretical calculations and by molecular beam scattering experiments. In addition, there are several phenomena due entirely to the angular part of the intermolecular potential. One of these is nuclear spin relaxation. These experiments yield information which is useful in refining potential surfaces, especially when used in conjunction with other data which are also sensitive to the angular dependence of the potential. Furthermore, spin relaxation measurements in the gas phase yield molecular reorientation and rotational energy transfer rates which are of interest in themselves for the interpretation of experiments involving molecular dynamics and energy disposal in the gas phase.

CO_2 has been chosen for relaxation studies for several reasons. CO_2 is an important component of the atmosphere. ^{13}C in CO_2 has a *single* relaxation mechanism (spin rotation) in the gas phase, therefore it is possible to extract collision cross sections from relaxation times. A linear molecule colliding with Ar, Kr, or Xe is a simple enough system for theoretical interpretation; for the atom–linear molecule collision pair, only rotational–translational energy transfer need be considered. CO_2 has a small rotational constant ($B_0 = 0.388\,703\ \text{cm}^{-1}$) so that classical or semiclassical collision theory can be used to attempt to reproduce the experimental data with an assumed potential function.[1] Other data which help define the potential surface are already available for the binary interaction of CO_2 and the other molecules used in this study.

Broadening coefficients and pressure broadening cross sections of specific rotational lines in the vibrational bands of CO_2 in a large number of buffer gases[2–7] which include those chosen for our spin relaxation studies (CO_2, N_2, Xe, O_2, Ar, Kr, and CH_4) have been reported and temperature- and J-dependent cross sections have been determined.[8,9] The absorption profiles of the ν_3 band of CO_2 in Ne, Ar, and Kr yield mean square torques which are used to determine the anisotropy in the repulsive part of the CO_2–rare gas potential.[10] Line shapes of collision-induced microwave, Raman, and depolarized Rayleigh spectra of CO_2 and their dependence on temperature and density are expected to be sensitive to the collision dynamics and the nature of the intermolecular forces.[11] Various CO_2 van der Waals complexes have been characterized spectroscopically, among them $(CO_2)_2$, CO_2–HF, CO_2–DF, CO_2–HCl, and CO_2–Ar.[12–15] The molecular constants of these complexes probe the well regions of the potentials. Reliable transport and virial coefficients for CO_2 and its mixtures are known.[16,17]

A potential function for CO_2–Ar constructed from a theoretical repulsive term and perturbation calculation of the dispersion part gives good agreement with second virial coefficients, transport properties, and beam differential scattering cross sections.[18] A multiple collision rainbow effect which has been observed in the scattering of CO_2 and Xe is found to be sensitive to the anisotropy of the potential and also the slope of the repulsive branch.[19] A CO_2–CO_2 potential function has been determined using a combination of theoretical and experimental data.[20]

In this work we provide the first spin relaxation studies in CO_2. These yield cross sections for rotational angular momentum changes in CO_2 in collisions with CO_2, CH_4, N_2, Ar, HCl, Kr, Xe, and SF_6 molecules as a function of temperature and are sufficiently precise to motivate further investigation of CO_2 potential energy surfaces.

 0021-9606/87/052717-06$02.10

EXPERIMENTAL

Isotopically labeled (90% ^{13}C) CO_2 from MSD Isotopes and buffer gases which were not isotopically labeled were used as obtained from vendors. The gas samples were prepared as in our previous gas phase NMR shielding studies.[21] Measurements were taken at 50.28 MHz on an IBM WP-200 (4.7 T) NMR spectrometer. The field was shimmed on the proton FID of a sealed tube of ethylene glycol or methanol which was also used as a temperature standard above or below room temperature, respectively. Sealed gas samples of known densities were placed in a standard 5 mm tube and the experiments were conducted without field-frequency lock since the field drift was less than 4 Hz per day and entirely unnoticeable in our experiments. Other experiments under field-frequency lock with the 5 mm tube in a 10 mm tube containing lock solvent (DMSO-d_6 for high temperature work, $CDCl_3$ for low temperatures) gave results indistinguishable from the data taken in the above mode of operation.

The standard inversion recovery ($5T_1$–π–τ–$\pi/2$) pulse sequence[22] for T_1 measurements was used. The intensity of the peak corresponding to delay time τ is given by

$$A_\tau = A_\infty [1 - \exp(-\tau/T_1)] + A_0 \exp(-\tau/T_1), \quad (1)$$

where A_0 is the intensity after a π pulse. Any slight deviation from $A_0 = -A_\infty$ due to B_1 (rf field) inhomogeneity is properly taken into account by the above form. A typical plot of $\ln[(A_\infty - A_\tau)/(A_\infty - A_0)]$ vs τ gives a slope of $-1/T_1$ as shown in Fig. 1. Densities used in this study are all in "the extreme narrowing limit" such that in pure CO_2 the spin-lattice relaxation time is proportional to the density ρ.

The temperature dependence of T_1/ρ has been studied for several pure gases in which relaxation is dominated by the spin-rotation mechanism and found to be consistent with the power law $(T_1/\rho) \propto T^{-n}$, where n is very nearly 3/2. For pure CO_2 a least squares fit of $\ln(T_1/\rho)$ vs $\ln(T/300)$ has a slope of -1.51 ± 0.05 and $(T_1/\rho)_{300} = 0.0216 \pm 0.0005$ s amagat^{-1}. For CO_2 in a buffer gas, relaxation by the spin rotation mechanism is caused by CO_2–CO_2 collisions and by CO_2–buffer collisions. In this study it is empirically established that these effects are additive in the density range 5–50 amagat, i.e.,

$$T_1 = \rho_{CO_2}\left(\frac{T_1}{\rho}\right)_{CO_2-CO_2} + \rho_{buffer}\left(\frac{T_1}{\rho}\right)_{CO_2\text{–buffer}}. \quad (2)$$

An example is shown in Fig. 2 where the CO_2–CO_2 contribution has been subtracted from the observed T_1 leaving the second term in Eq. (2), which is evidently directly proportional to the density of the buffer gas. Several samples of gas mixtures with constant small amounts of CO_2 (~ 8 amagat) and varying larger amounts of buffer (25–40 amagat) were used. The linear dependence on density was verified for each CO_2–buffer pair. The density of CO_2 in each sample is large enough to give a good signal to noise ratio and still small enough to minimize errors in $(T_1/\rho)_{CO_2\text{–buffer}}$ caused by subtraction of quantities of similar magnitude in Eq. (2). The temperature dependence of $(T_1/\rho)_{CO_2\text{–buffer}}$ is fit to the form of Eq. (3):

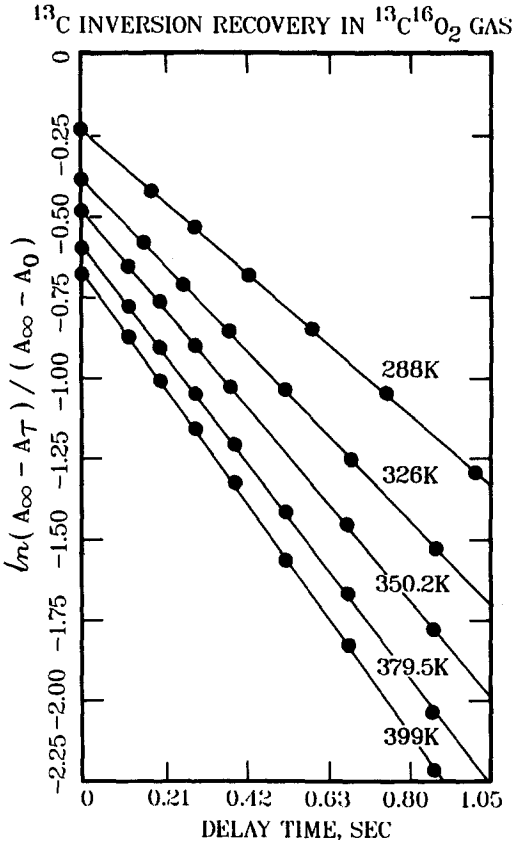

FIG. 1. Typical data for ^{13}C inversion recovery experiment in pure $^{13}CO_2$ gas (41 amagat). (The ordinate of each curve has been displaced in order that the different curves may be displayed in the same figure.) The slope of each line is $-1/T_1$.

$$\left(\frac{T_1}{\rho}\right) = \left(\frac{T_1}{\rho}\right)_{300\,K}\left(\frac{T}{300}\right)^{-n}. \quad (3)$$

The effect of oxygen as a buffer gas was also determined; the results will be published separately. However, inadvertent contamination by small amounts of oxygen do not affect the results in this study.

RESULTS

Figure 3 shows the temperature dependence of T_1 for CO_2 in various buffers. The lines are not all parallel, indicating different temperature dependences for different buffer gases. The numerical results are given for each buffer in Table I. The exponent $-n$ differs from the expected -1.5 outside of experimental error for CO_2 in buffer gases CH_4, Ar, Kr, and N_2.

Cross sections for rotational angular momentum transfer σ_J were found by using Gordon's theory[23]:

$$\left(\frac{T_1}{\rho}\right) = \frac{3\bar{v}}{2\langle J(J+1)\rangle C_\perp^2}\sigma_J(T)$$

$$\approx \frac{3B_0}{2kTC_\perp^2}\left(\frac{8kT}{\pi\mu}\right)^{1/2}\sigma_J(T). \quad (4)$$

B_0 is the rotational constant and $C_\perp$ is the spin rotation con-

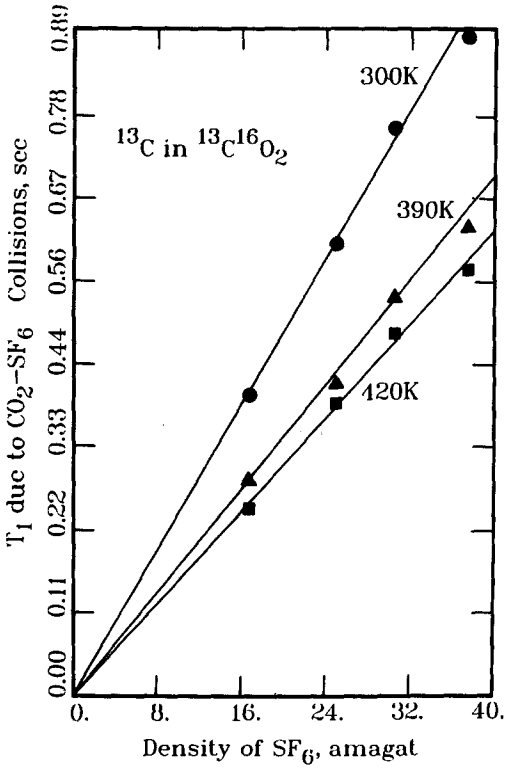

FIG. 2. Typical data verifying that a characteristic (T_1/ρ) due to CO_2-buffer collisions may be extracted from the relaxation time of the mixture as given in Eq. (3).

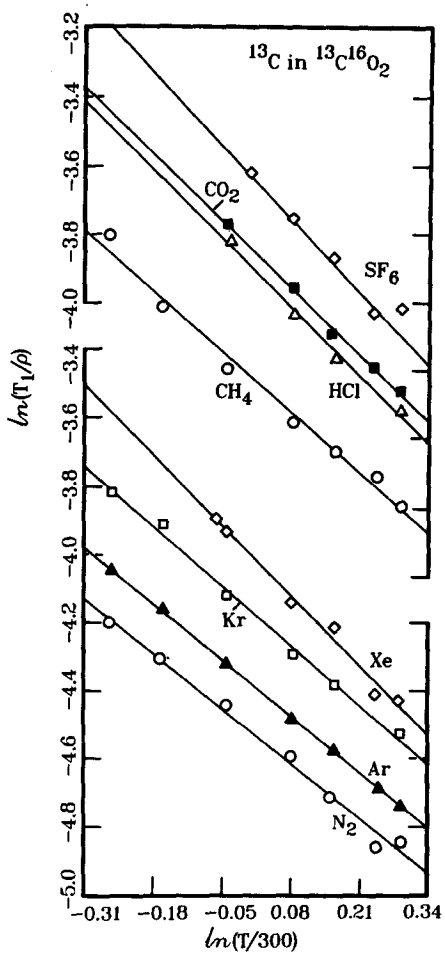

FIG. 3. The temperature dependence of (T_1/ρ) of ^{13}C in CO_2 in various gases in the extreme narrowing limit.

stant, which is 5.30 kHz for $^{13}CO_2$.[24] The cross sections calculated from (T_1/ρ) at 300 K are given in Table II for each molecular pair.

In Gordon's classical theory the cross section is defined as

$$\sigma_J(T) = \frac{1}{2\langle J^2\rangle}\int_0^\infty \langle(\mathbf{J}_f - \mathbf{J}_i)^2\rangle 2\pi b\, db, \qquad (5)$$

where $\mathbf{J}_i$ and $\mathbf{J}_f$ are the angular momentum vectors before and after a collision; and the average $\langle\ \rangle$ is taken over both the distribution of internal states before a collision and the initial distribution of relative velocities. For CO_2 in CH_4, N_2, Ar, and Kr, the temperature dependence of T_1 differs from the expected $T^{-3/2}$. This implies that the cross section $\sigma_J(T)$ has a temperature dependence significantly different from the explicit T^{-1} behavior of $1/\langle J^2\rangle^T$. For these collision pairs, it is possible to determine the temperature dependence of the collision integral $\frac{1}{2}\int\langle\Delta J^2\rangle 2\pi b\, db$. We express the latter as

$$\frac{1}{2\langle J^2\rangle_{300\,\mathrm{K}}}\int_0^\infty \langle\Delta J^2\rangle 2\pi b\, db$$
$$= \frac{T}{300}\sigma_J(T) = \sigma_J(300\,\mathrm{K})[1 + a_1(T-300)], \quad (6)$$

as shown in Fig. 4. The collision integral is temperature independent (or has a very weak temperature dependence) in CO_2–CO_2, CO_2–HCl, CO_2–Xe, and CO_2–SF_6, and increases with increasing temperature in CO_2–CH_4, CO_2–N_2, CO_2–Ar, and CO_2–Kr.

DISCUSSION

The geometric cross sections $\sigma_{\mathrm{geom}} = \pi r_0^2$ of each collision pair are given in Table III. The ratios $\sigma_J/\sigma_{\mathrm{geom}}$ are close to 1, indicating a high efficiency of rotational angular momentum transfer; every one or two "hard sphere" collisions results in reorientation or a change in rotational energy. Table III shows that the efficiency of collisions increases with increasing electric dipole polarizability, except for the unusually high values for CO_2–CO_2 and CO_2–HCl.

For a $D_{\infty h}$ molecule such as CO_2 with a linear collision partner, the induction term is negligible and the electrostatic and dispersion terms are as follows[25]:

TABLE I. Spin relaxation times for ^{13}C in CO_2 with various buffers[a]: $T_1 = (T_1/\rho)_{300\,\mathrm{K}}\cdot\rho\cdot(T/300)^{-n}$.

Buffer	$(T_1/\rho)_{300\,\mathrm{K}}$, ms amagat^{-1}	n
CH_4	14.9 ± 0.5	1.36 ± 0.07
N_2	10.9 ± 0.3	1.24 ± 0.06
Ar	12.6 ± 0.09	1.27 ± 0.01
HCl	20.5 ± 0.5	1.6 ± 0.1
CO_2	21.6 ± 0.3	1.51 ± 0.05
Kr	15.6 ± 0.3	1.35 ± 0.04
Xe	18.4 ± 0.6	1.6 ± 0.1
SF_6	27 ± 2	1.6 ± 0.2

[a] Temperature range is 290–400 K, except for CO_2 in CH_4 and SF_6 where it is 230–400 K and 300–400 K, respectively.

$$U_{\text{elec}} = \tfrac{3}{2}\mu_2\Theta_1 R^{-4}[\cos\theta_2(3\cos^2\theta_1 - 1) + 2\sin\theta_1\cos\theta_1\sin\theta_2\cos\phi]$$
$$+ \tfrac{3}{4}\Theta_1\Theta_2 R^{-5}[1 - 5\cos^2\theta_1 - 5\cos^2\theta_2 + 17\cos^2\theta_1\cos^2\theta_2$$
$$+ 2\sin^2\theta_1\sin^2\theta_2\cos^2\phi + 16\sin\theta_1\cos\theta_1\sin\theta_2\cos\theta_2\cos\phi + \cdots], \quad (7)$$

$$U_{\text{disp}} = -[3U_1U_2/2(U_1+U_2)]R^{-6}[\alpha_1\alpha_2 + \tfrac{1}{3}\alpha_1(\alpha_\parallel - \alpha_\perp)_2$$
$$\times(\tfrac{3}{2}\cos^2\theta_2 - \tfrac{1}{2}) + \tfrac{1}{3}\alpha_2(\alpha_\parallel - \alpha_\perp)_1(\tfrac{3}{2}\cos^2\theta_1 - \tfrac{1}{2}) + 2\alpha_1A_{2\parallel}R^{-1}\cos^3\theta_2 + 2\alpha_2A_{1\parallel}R^{-1}\cos^3\theta_1$$
$$+ \tfrac{4}{3}\alpha_1A_{2\perp}R^{-1}(3\cos\theta_2 - 2\cos^3\theta_2) + \tfrac{4}{3}\alpha_2A_{1\perp}R^{-1}(3\cos\theta_1 - 2\cos^3\theta_1) + \cdots], \quad (8)$$

where subscripts 1 and 2 refer to CO_2 and collision partner, respectively. The increasing order of collision efficiencies according to polarizability is therefore an indication that these cross sections provide information about the anisotropy arising from the dispersion terms. The unusually high efficiency of CO_2–CO_2 and CO_2–HCl collisions can be attributed to the anisotropy of U_{elec} terms. CO_2 has a large quadrupole moment, -4.2 buckingham[25] compared to 1.5 for N_2, hence there is a large R^{-5} contribution to the CO_2–CO_2 pair potential. CO_2 is also a more efficient collision partner for rotational energy exchanges due to matching of rotational energy levels of the collision pair. For CO_2–HCl the leading term in R^{-4} is important because of the large dipole moment of HCl. The fairly good correlation of the collision efficiencies with magnitudes of electrical moments and polarizabilities seem to indicate the sensitivity of the cross sections σ_J to the attractive part of the potential. Collision dynamics calculations using interaction potentials now available for CO_2–Ar, Xe are expected to test both the repulsive and attractive parts of the potential with the temperature dependence of σ_J. The form of the temperature dependence is not necessarily T^{-n}, but Fig. 3 shows that our data are consistent with this form.

Cross sections for spin rotation relaxation and electric dipole absorption provide complementary information; they involve slightly different sigma matrices thus reflecting somewhat different characteristics of the same potential.[1] Pressure broadening cross sections, σ_{IR}, have been reported for CO_2 and are shown in Table IV. The repeatability of linewidth measurements is inferior to relaxation measurements using pulse methods as is clearly demonstrated in determinations of T_1 and T_2 in NMR by both techniques. Pressure broadening data have this disadvantage. Note the discrepancies in reported cross sections for the same rotational line for a given pair, even in the pure CO_2 data where no contributions from other types of collisions need be subtracted from the observed linewidth. The reported cross sections for the same $P(20)$ line of the 10.6 μm transition in pure CO_2 range from 136 to 200 Å^2. The poor reproducibility can be attributed to instrumental line broadening. However, these cross sections do have the important advantage of being labeled according to the J quantum number of the initial state and thus they provide even more detailed information than a temperature dependent thermal average cross section.

The collision efficiencies from pressure broadening data[2] roughly follow the same ordering as the spin relaxation efficiencies, with some exceptions. Nielsen and Gordon[1] have found that pressure broadening cross sections are highly dependent on inelastic collisions and much less so on elastic collisions, while spin relaxation cross sections are dominated by elastic collisions. The pressure broadening

TABLE II. Cross sections for rotational angular momentum transfer in CO_2 due to collisions with various buffer molecules[a]: $\sigma_J(T) = \sigma_J(300\text{ K})\cdot(T/300)^{-m} \simeq \sigma_J(300\text{ K})\,(300/T)\,[1 + a_1(T-300)]$.

Buffer	m	$\sigma_J(300\text{ K})$, Å^2	a_1, deg^{-1}
CH_4	0.86 ± 0.07	30 ± 1	0.014 ± 0.006
N_2	0.74 ± 0.06	26.6 ± 0.8	0.0226 ± 0.005
Ar	0.77 ± 0.01	33.9 ± 0.2	0.0254 ± 0.0013
HCl	1.1 ± 0.1	53.5 ± 0.9	⋯
CO_2	1.01 ± 0.05	59.9 ± 0.8	⋯
Kr	0.63 ± 0.04	49 ± 1	0.026 ± 0.007
Xe	1.1 ± 0.1	62 ± 2	⋯
SF_6	1.1 ± 0.2	91 ± 3	⋯

[a] The temperature ranges are the same as in Table I.

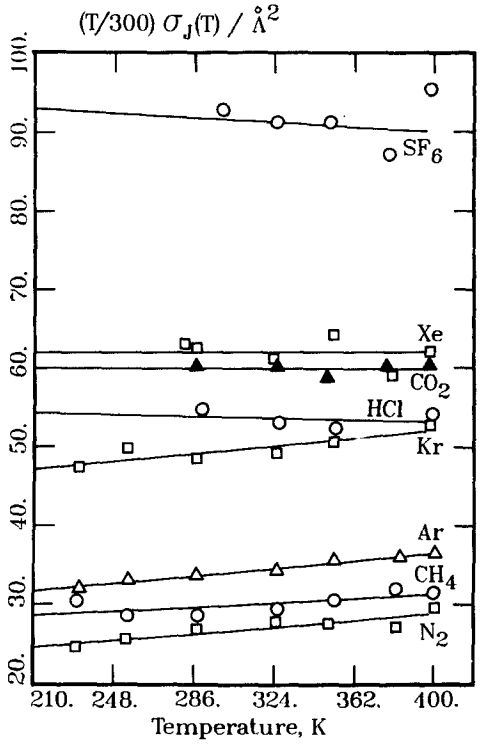

FIG. 4. The temperature dependence of $(1/2\langle J^2\rangle_{300})\int_0^\infty \langle\Delta J^2\rangle 2\pi b\,db$ is given by $(T/300)\sigma_J(T)$. The data are fitted to a linear equation $\sigma_J(300\text{ K}) \times [1 + a_1(T\text{-}300)]$ with no theoretical or physical basis, merely that the quality of the data over the temperature range does not justify any other functional form.

TABLE III. Geometric cross sections and collision efficiencies for CO_2 with various buffers.

Buffer	r_0(pair)[a], Å	σ_{geom}, Å^2	σ_J, Å^2	σ_J/σ_{geom}
CH_4	3.727	43.64	30	0.69
N_2	3.705	43.13	26.6	0.62
Ar	3.604	40.80	33.9	0.83
HCl	3.554	39.68	53.5	1.35
CO_2	3.769	44.63	59.9	1.34
Kr	3.633	41.47	49	1.2
Xe	3.843	46.40	62	1.4
SF_6	4.426	61.54	91	1.5

[a] From G. C. Maitland, M. Rigby, E. B. Smith, and W. A. Wakeham, *Intermolecular Forces* (Clarendon, Oxford, 1981), Table A3.2, except for CO_2–HCl and CO_2–Xe which were calculated from the arithmetic mean of r_0 for the like pairs, from Table A3.2 and A. F. Turfa and R. A. Marcus, J. Chem. Phys. **70**, 3035 (1979).

efficiencies are thus dependent upon the mass of the perturber (heavier perturbers are more likely to cause J-changing collisions).[2] Since the ordering of buffer molecules according to mass and polarizability are not independent, it is difficult to determine which one is dominant in determining collision efficiencies from pressure broadening. Since J-changing collisions would be more likely to occur between a pair of molecules with matching rotational energy levels, the efficiency of CO_2–CO_2 collisions is even more pronounced in the pressure broadening data than in the spin relaxation data. Thus the pressure broadening collision efficiencies are $Ar < Kr < Xe < CO_2$,[2,4] while the spin relaxation collision efficiencies are in the order $Ar < Kr < CO_2 < Xe$. The unusually large CH_4–CO_2 collision efficiency in pressure broadened data has been explained as being due to resonance of the ν_4 vibrational mode of CH_4 with the 10.6 μm transition of CO_2.[2]

TABLE IV. Pressure broadening cross sections for the $P(20)$ line of the 10.6 μm transition of CO_2 in various buffers at room temperature.

Buffer	σ_{IR}, Å^2	Ref.	$\sigma_{IR}/\sigma_{geom}$	σ_J/σ_{geom}
CH_4	148 ± 7	2	3.39	0.69
N_2	120 ± 6	2	2.78	0.62
	87.6	5	2.03	
	87.2	6	2.02	
	57.1[a]	9	1.32	
	89.5 ± 3.5[b]	4	2.07	
Ar	90 ± 5	2	2.21	0.83
	107	5	2.62	
	83.3 ± 3.5[b]	4	2.04	
CO_2	157 ± 8	2	3.52	1.34
	136	5	3.04	
	137	6	3.07	
	200	3	4.48	
	149	7	3.34	
	75.5[a]	9	1.69	
	126.9 ± 5[b]	4	2.84	
Kr	108 ± 5	2	2.60	1.2
Xe	151 ± 8	2	3.25	1.4
	115.3 ± 4.7[b]	4	2.48	

[a] $R(20)$ line of 4.2 μm transition.
[b] 2.7 μm transition.

CONCLUSIONS

The cross sections obtained in this study are thermal average total cross sections for J-changing and m_J-changing collisions. These immediately provide information about the range of the effective interaction between CO_2 and collision partner, and are compared with the analogous parameters derived from other experiments. The small CO_2–N_2 and CO_2–CH_4 cross sections indicate that collisions which result in CO_2 molecular reorientation and rotational energy transfer are relatively short-range interactions, which suggests that the anisotropy in the repulsive branch of the interaction potential must be involved. On the other hand, the large CO_2–Xe and CO_2–SF_6 cross sections suggest that dispersion terms are very important for these collision couples.

The temperature dependence exhibited by CO_2–N_2, CO_2–Ar and CO_2–Kr cross sections deviate significantly from the T^{-1} behavior, i.e., the collision integral $\frac{1}{2}\int_0^\infty \langle(\Delta \mathbf{J})^2\rangle 2\pi b\, db$ is temperature dependent. This supports the short range nature of the interactions that contribute to σ_J. On the other hand, the corresponding pressure broadening cross sections are 2–5 times larger, indicating that longer-range interactions are relatively more important than short-range ones compared to spin relaxation, which in turn, justifies the use of linewidths of rotational lines in IR bands for determinations of electrical moments.

ACKNOWLEDGMENT

This research was supported in part by the National Science Foundation (CHE85-05725).

[1] W. B. Nielsen and R. G. Gordon, J. Chem. Phys. **58**, 4131, 4149 (1973).
[2] T. W. Meyer, C. K. Rhodes, and H. A. Haus, Phys. Rev. A **12**, 1993 (1975).
[3] P. J. Francisco, C. Valero, B. Suarez, and R. W. Boese, J. Quantum Spectrosc. Radiat. Transfer **23**, 337 (1980).
[4] D. F. McLaughlin and A. T. Mattick, J. Quantum Spectrosc. Radiat. Transfer **27**, 611 (1982).
[5] T. K. McCubbin and T. R. Mooney, J. Quantum Spectrosc. Radiat. Transfer **8**, 1255 (1968).
[6] R. L. Abrams, Appl. Phys. Lett. **25**, 609 (1974).
[7] E. Arie, N. Lacombe, and C. Rossetti, Can. J. Phys. **50**, 1800 (1972).
[8] G. L. Tettemer and W. G. Planet, J. Quantum. Spectrosc. Radiat. Transfer **24**, 343 (1980).
[9] H. Oodate and T. Fujioka, J. Chem. Phys. **68**, 5494 (1978).
[10] L. Berreby and E. Dayan, Mol. Phys. **48**, 581 (1983); C. Dreyfus, L. Berreby, and E. Dayan, Chem. Phys. Lett. **79**, 476 (1981).
[11] A. A. Maryott and G. Birnbaum, J. Chem. Phys. **36**, 2026 (1962); P. A. Madden and T. I. Cox, Mol. Phys. **56**, 223 (1985); C. S. Murthy, R. Vallauri, H. Versmold, U. Zimmermann, and K. Singer, Ber. Bunsenges. Phys. Chem. **89**, 18 (1985).
[12] R. E. Miller and R. O. Watts, Chem. Phys. Lett. **105**, 409 (1984); G. A. Pubanz, M. Maroncelli, and J. W. Nibler, *ibid.* **120**, 313 (1985).
[13] J. A. Shea, W. G. Read, and E. J. Campbell, J. Chem. Phys. **79**, 614 (1983); L. Andrews, R. T. Arlinghaus, and G. L. Johnson, *ibid.* **78**, 6353 (1983).
[14] J. M. Steed, T. A. Dixon, and W. Klemperer, J. Chem. Phys. **70**, 4095 (1979).
[15] N. Fourati, B. Silvi, and J. P. Perchard, J. Chem. Phys. **81**, 4737 (1984).
[16] J. Kestin, S. T. Ro, and Y. Nagasaka, Ber. Bunsenges. Phys. Chem. **86**, 945 (1982); H. L. Robjohns and P. J. Dunlop, *ibid.* **85**, 655 (1981).
[17] J. H. Dymond and E. B. Smith, *The Virial Coefficients of Pure Gases and Mixtures* (Oxford University, New York, 1980).
[18] G. D. Billing, Chem. Phys. **91**, 327 (1984).
[19] U. Buck, F. Huisken, D. Otten, and R. Schinke, Chem. Phys. Lett. **101**,

126 (1983); U. Buck, D. Otten, R. Schinke, and D. Poppe, J. Chem. Phys. **82**, 202 (1985).
[20]H. J. Böhm, R. Ahlrichs, P. Scharf, and H. Schiffer, J. Chem. Phys. **81**, 1389 (1984).
[21]C. J. Jameson, A. K. Jameson, and S. M. Cohen, J. Chem. Phys. **62**, 4224 (1975).
[22]R. L. Vold, J. S. Waugh, M. P. Klein, and D. E. Phelps, J. Chem. Phys. **48**, 3831 (1968).
[23]R. G. Gordon, J. Chem. Phys. **44**, 228 (1966)
[24]R. D. Amos and M. B. Battaglia, Mol. Phys. **36**, 1517 (1978).
[25]A. D. Buckingham, Adv. Chem. Phys. **12**, 107 (1967).